Available online at www.sciencedirect.com
ScienceDirect
Journal of the European Ceramic Society 31 (2011) 637–644
www.elsevier.com/locate/jeurceramsoc

In situ synthesis and densification of submicrometer-grained B_4C–TiB_2 composites by pulsed electric current sintering

S.G. Huang, K. Vanmeensel, O. Van der Biest, J. Vleugels *

Department of Metallurgy and Materials Engineering, Katholieke Universiteit Leuven, Kasteelpark Arenberg 44, B-3001 Heverlee, Leuven, Belgium

Received 31 May 2010; received in revised form 12 October 2010; accepted 27 October 2010
Available online 27 November 2010

Abstract

B_4C composites with 15 and 30 vol% TiB_2 were pulsed electric current sintered from B_4C–TiO_2–carbon black mixtures in vacuum at 2000 °C. Full densification could be realised when applying an optimized loading cycle in which the maximum load is applied after completion of the B_4C–TiB_2 powder synthesis, allowing degassing of volatile species. The influence of the sintering temperature on the phase constitution and microstructure during synthesis and densification was assessed from interrupted sintering cycles. The in situ conversion of TiO_2 to TiB_2 was a complex process in which TiO_2 is initially converted to TiB_2 with B_2O_3 as intermediate product at 1400–1700 °C. At 1900–2000 °C, B_2O_3 reacted with C forming B_4C and CO. The B_4C and TiB_2 grain size in the fully densified 30 vol% TiB_2 composite was 0.97 and 0.63 μm, combining a Vickers hardness of 39.3 GPa, an excellent flexural strength of 865 MPa, and modest fracture toughness of 3.0 MPa $m^{1/2}$.

Keywords: Pulsed electric current sintering; Borides; Powders-solid state reaction; Grain size; C. Mechanical properties

1. Introduction

As one of the hardest materials known, boron carbide ranks third behind diamond and cubic boron nitride. Being intrinsically brittle, B_4C often requires different additives to improve its sintering behaviour and mechanical properties. Numerous researchers have shown that the addition of TiB_2 to B_4C can decrease the porosity level and improve the fracture toughness as well as flexural strength.[1–6] Furthermore, dense B_4C–TiB_2 composites can be easily machined using electrical discharge machining (EDM) since TiB_2 has a good electrical conductivity.[7–10] Since both B_4C and TiB_2 are covalently bonded compounds, sintering temperatures above 2200 °C were required for pressureless sintering of B_4C–TiB_2 particulate composites.[1,3] However, rapid grain growth and concomitantly decreased strength were observed in pressureless liquid phase sintered B_4C–TiB_2 composites. A recent study showed that hot pressing and pulsed electric current sintering aided in increasing the density of TiB_2 while decreasing the sintering time.[11,12]

Another way to make B_4C–TiB_2 composites is via in situ reaction of TiO_2, carbon and B_4C[3–5] or from elemental powders.[13] A flexural strength of 866 MPa and fracture toughness of 3.2 MPa $m^{1/2}$ were reported for fully dense B_4C-20 mol% (15 vol%) TiB_2 composites made from B_4C, TiO_2 and carbon black mixtures prepared by reaction hot pressing for 1 h at 2000 °C under a pressure of 50 MPa.[5] In situ TiB_2 formation is reported when sintering B_4C with TiO_2 or Ti addition in the 1800–2190 °C range.[14] A mixture of fine-sized B_4C with 40 wt% TiO_2 was transformed into a 95% dense B_4C–TiB_2 composite when sintering for 1 h at 2160 °C.[14] More recently, pseudo-eutectic micrometer grained TiB_2–B_4C composites were synthesized by PECS of mechanically alloyed elemental powders at 1200–1700 °C.[13] Phase formation was completed well before full density was achieved and bulk composite materials of nearly full density were obtained when PECS at 1700 °C.[13]

In the present study, B_4C–TiB_2 composites with up to 30 vol% TiB_2 were made by in situ synthesis from B_4C, TiO_2 and carbon black powder mixtures during densification by pulsed electric current sintering (PECS). The effect of the processing temperature on the densification, phase constitution, as well as microstructure of the sintered compacts was assessed.

* Corresponding author. Tel.: +32 16 321244; fax: +32 16 321992.
E-mail address: jozef.vleugels@mtm.kuleuven.be (J. Vleugels).

0955-2219/$ – see front matter © 2010 Elsevier Ltd. All rights reserved.
doi:10.1016/j.jeurceramsoc.2010.10.028

2. Experimental procedure

2.1. Material preparation

B_4C–TiB_2 composites were made by in situ reaction of B_4C (Grade HD20, H.C. Starck, Germany, $d_{50} = 0.5\,\mu m$), TiO_2 (Grade A-HR, Huntsman Tioxide Europe Ltd., crystal size = 0.17 μm) and carbon black (Grade 4, Degussa; Germany) powders. Composites B15T and B30T with a desired TiB_2 content of 15 and 30 vol% respectively were prepared by low energy multidirectional mixing (Turbula T2A, WAB, Switzerland) in ethanol for 24 h using ZrO_2 milling balls ($\phi = 5$ mm, grade TZ-3Y, Tosoh, Japan). The solvent was removed in a rotating evaporator at 65 °C and the powder mixture was additionally dried for 24 h at 80 °C. The starting compositions were determined so as to form B_4C matrix composites with 15 or 30 vol% TiB_2, which have a theoretical density of 2.82 and 3.12 g/cm^3 respectively, according to the rule of mixtures based on a density of 2.52 and 4.52 g/cm^3 for B_4C and TiB_2. The formation of TiB_2 phase can be described according to[3,4]:

$$B_4C + 2TiO_2 + 3C \Leftrightarrow 2TiB_2 + 4CO \quad (1)$$

Under standard state conditions, the change in Gibbs free energy of this reaction can be expressed as: $\Delta G = 732.7–6.5\,T$ (kJ), which is thermodynamically favourable at temperatures above 1150 °C.[14] Reaction (1) proceeds more rapidly when the CO partial pressure is below the equilibrium pressure, i.e. in vacuum or Ar atmosphere. In the absence of free carbon, TiO_2 can be converted to TiB_2 using B_4C as carbon source.[14–17]

In the present study, in situ powder synthesis and sintering was performed during PECS (Type HP D 25/1, FCT Systeme, Rauenstein, Germany) in a vacuum of 4 mbar. A pulsed electric current was applied with a pulse duration of 10 ms and pause time of 5 ms throughout all the experiments. Powder mixtures were poured into a cylindrical graphite die with an inner and outer diameter of 30 and 56 mm. The B30T powder mixture was PECS at 1400, 1700, 1900 and 2000 °C for 5–13 min, including outgassing, pressure loading and dwell time at the sintering temperature, under a maximum pressure of 60 MPa, with a heating and initial cooling rate of 200 °C/min. A representative thermal cycle is given in Fig. 1 for the powder mixture heated for 9 min at 2000 °C. In all experiments, a minimum pressure of 8 MPa was applied to ensure constant contact of the electrodes with the die/punch/sample system. Two different loading cycles were investigated. In loading cycle C1, the pressure was gradually increased from 8 to 60 MPa within 1 min upon reaching 2000 °C. In the optimized cycle C2, the maximum pressure of 60 MPa was applied within 1 min, 4 min after reaching 2000 °C allowing degassing of volatile species. Graphite paper was used to separate the graphite die/punch set-up and powder mixture. A 10 mm thick porous carbon felt insulation was placed around the graphite die to obtain a homogeneous temperature distribution and concomitant sintering behaviour. The sintering temperature was measured by a two-colour pyrometer (400–2300 °C, Impac, Chesterfield, UK), focused at the bottom of a central borehole in the upper punch, 2 mm away from the top surface of the sample. The actual set-up and temperature monitoring procedure is described in detail elsewhere.[18]

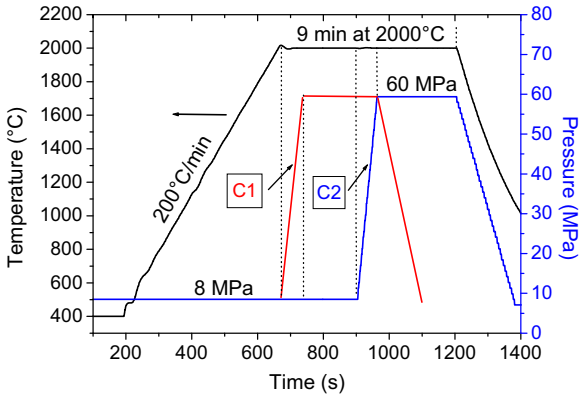

Fig. 1. Thermal and mechanical loading cycles during in situ synthesis and consolidation of B_4C–TiO_2–C starting powder mixtures without (C1) and with (C2) a degassing step upon reaching the targeted sintering temperature.

2.2. Characterization

After PECS and sand blasting, the sintered 4 mm thick discs were cross-sectioned and polished to a mirror finish. The bulk density of the sintered composites was measured in ethanol. The crystalline phases during the reaction were investigated by a θ–θ X-ray diffractometer (XRD, Seifert, Ahrensburg, Germany) using Cu-K_α radiation (40 kV, 40 mA). The microstructure and composition of the PECS materials were examined by scanning electron microscopy (SEM, XL30-FEG, FEI, Eindhoven, the Netherlands), equipped with an energy dispersive analysis system (EDS, EDAX, Tilburg, the Netherlands) for compositional analysis. The Vickers hardness, HV_1, was measured (Model FV-700, Future-Tech Corp., Tokyo, Japan) with an indentation load of 9.81 N. The fracture toughness, K_{IC}, was calculated from the length of the radial cracks of the indentations according to the formula of Anstis et al.[19] The elastic modulus, E, of the B_4C–TiB_2 composites was measured on rectangular bars by the resonance frequency method.[20] The resonance frequency was measured by the impulse excitation technique (Grindo-Sonic, Lemmens N.V., Leuven, Belgium). The flexural strength at room temperature was measured in a three-point bending test (Series IX Automated Materials Testing System 1.29, Instron Corporation) with a span width of 20 mm and a crosshead displacement of 0.1 mm/min on rectangular (25 mm × 3 mm × 2 mm) bars, which were cut from the PECS discs by electrical discharge machining. All surfaces were ground (grinding wheel type D46SW-50-X2, Technodiamant, The Netherlands) on a Jung grinding machine (JF415DS, Göppingen, Germany). The reported flexural strength values are the mean and standard deviation of five measurements.

3. Results and discussion

3.1. In situ synthesis of B_4C–TiB_2 powder

In the present study, a heating rate of 200 °C/min was applied to in situ synthesize TiB_2 and densify B_4C–TiB_2 composite

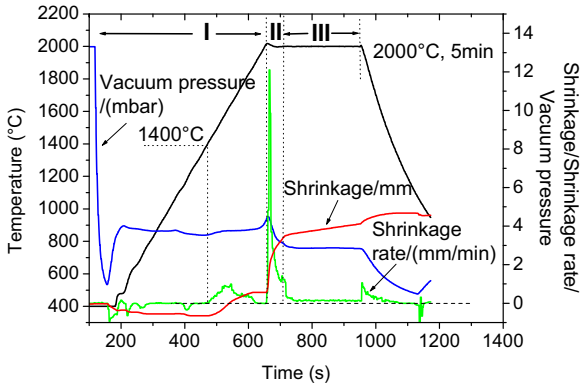

Fig. 2. Sintering behaviour of the B_4C–TiO_2–C powder mixture (B_4C-30 vol% TiB_2) during PECS for 6 min at 2000 °C under a pressure of 60 MPa without degassing step (cycle C1 in Fig. 1).

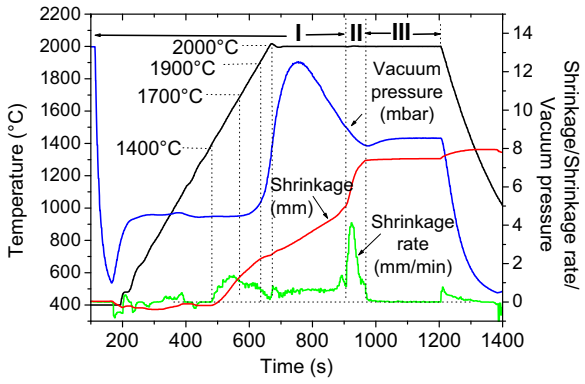

Fig. 3. Sintering behaviour of the B_4C–TiO_2–C powder mixture (B_4C-30 vol% TiB_2) during PECS for 9 min at 2000 °C under a pressure of 60 MPa with degassing step (cycle C2 in Fig. 1).

powders in one step using PECS. According to Eq. (1), the carbothermal reaction of TiO_2, C and B_4C produces a large amount of CO gas during TiB_2 powder synthesis. During PECS, the evolution of the vacuum pressure in the furnace and the shrinkage and shrinkage rate of the powder compacts were recorded to allow elucidating the reactive synthesis and densification process.

A representative thermal cycle for in situ synthesis and sintering of B_4C-30 vol% TiB_2 composites using loading cycle C1 is shown in Fig. 2. The complete cycle with a total duration of <25 min can be divided into three main steps, i.e., heating of the starting powder mixture, in situ synthesis of a B_4C–TiB_2 powder mixture and composite densification. After an initial thermal expansion of the powder compact, shrinkage starts around 1400 °C during the heating up phase (section I) before increasing the mechanical load. An abrupt increased shrinkage however is realised when applying a maximum pressure of 60 MPa within 1 min immediately upon reaching 2000 °C (section II). The compact further shrinks throughout the subsequent dwell period of 4 min at 2000 °C (section III). Upon increasing the load at 2000 °C, an increased vacuum pressure is observed implying the release of volatile species. The density of the sintered compact was only 85%.

In a second approach, presented in Fig. 3, the load was only increased after the maximum in vacuum pressure allowing outgassing of the volatile species (loading cycle C2 in Fig. 1). Besides a continuous shrinkage of the powder compact above 1400 °C, a sharp increase in vacuum pressure was observed starting around 1750 °C, as shown in section I of Fig. 3. The vacuum pressure reached a maximum after 1.5 min at 2000 °C. Note that the external pressure was kept at a minimum of 8 MPa for 4 min at 2000 °C in order to ensure that the in situ formed gas could leave the powder compact. After the measured vacuum pressure decrease about 4 min after reaching 2000 °C, the mechanical pressure was increased from 8 to 60 MPa within 1 min (section II in Fig. 2) resulting in a rapid shrinkage of the powder compact and a further decrease of the vacuum pressure. No further densification was observed after the load increase at 2000 °C as demonstrated by the constant displacement curves in section III in Fig. 3.

To assess the influence of the sintering temperature on the synthesis process, additional PECS cycles were conducted at 1400, 1700 and 1900 °C for the 30 vol% TiB_2 composite. The maximal pressure of 60 MPa was only applied after degassing a few minutes at 1400, 1700 and 1900 °C. The evolution of the vacuum pressure and densification as a function of temperature for the 15 and 30 vol% TiB_2 composites was comparable.

The bulk and relative density of the in situ synthesized B_4C–TiB_2 composites are summarized in Table 1. The densification behaviour exhibits a gradual increase in sintered density with increasing PECS temperature from 1400 to 2000 °C. With degassing step, the B15T and B30T composites PECS at 2000 °C reached full densification, whereas a relative density of only 85% was obtained for the B30T composite processed without degassing step.

The XRD patterns of the B30T starting powder and the fractured and ground surfaces of the composites PECS at 1400, 1700, 1900 and 2000 °C are compared in Fig. 4. The JCPDS cards matching the spectra are 84-1286 for anatase TiO_2, 86-1129 for rhombohedral B_4C, 85-2083 for hexagonal TiB_2, 73-2158 for H_3BO_3, and 41-1487 for hexagonal graphite. Since the C source is amorphous carbon black, only TiO_2 and B_4C phases were found in the starting powder.

The XRD patterns and accompanying Rietveld quantification analysis (Table 1) reveal full conversion of TiO_2 to hexagonal TiB_2 after PECS for 7 min degassing + 5 min dwell at 1400 °C or 5.5 degassing + 5 min dwell at 1700 °C. However, there was no noticeable vacuum drop during these thermal cycles, implying that there is a non-volatile oxygen-containing intermediate product involved.

According to the Rietveld analysis (Table 1), the TiB_2 phase content remained almost constant in the powder compacts PECS at 1400, 1700, 1900 and 2000 °C with a degassing step. The B_4C content on the other hand gradually increased with increasing PECS temperature. Beside the aforementioned phases, diffraction peaks from graphite and H_3BO_3 phases were identified in the ceramics PECS at 1400, 1700 and 1900 °C. The carbon black remained amorphous at 1400 °C and transformed to graphite at 1700 and 1900 °C. An intense H_3BO_3 peak at 28° 2θ was observed on the fractured surfaces of the ceramics PECS at 1400,

Table 1
PECS parameters and phase constitution of the in situ PECS synthesized B_4C–TiB_2 composites.

Grade	Tempe-rature (°C)	Degassing time (min)	Dwell time (min)	ρ (g/cm^3)	R.D. (%)	Oxygen content (wt%)	Constituent phases (wt%)[a]
B30T	Powder	–	–	–	–	16.9 ± 0.6	37.1 TiO_2 + 54.7 B_4C + 8.1 Amorphous C
	1400	7	5	2.29	73.0	16.8 ± 1.8	43.7 TiB_2 + 38.8 B_4C + 17.5 H_3BO_3 + Amorphous C
	1700	5.5	5	2.56	82.0	16.4 ± 0.7	41.1 TiB_2 + 39.5 B_4C + 9.6 H_3BO_3 + 9.8 Graphite
	1900	4	5	3.01	96.6	2.5 ± 0.4	41.1 TiB_2 + 52.2 B_4C + 3.8 H_3BO_3 + 0.6 Graphite
	2000	4	5	3.16	100	1.2 ± 0.3	43.1 TiB_2 + 56.9 B_4C
	2000	0	5	2.65	85.0	8.4 ± 1.6	37.1 TiB_2 + 42.0 B_4C + 0.7 H_3BO_3 + 20.3 Graphite
B15T	2000	4	5	2.84	100	0.2 ± 0.1	78.3 TiB_2 + 21.7 B_4C

[a] As obtained by Rietveld analysis.

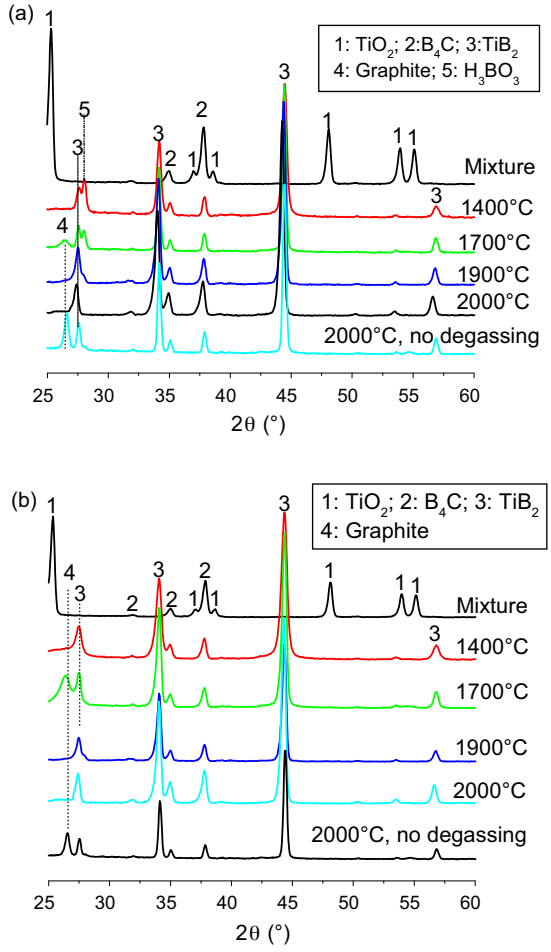

Fig. 4. XRD patterns of the starting powder mixture and fracture (a) and ground (b) surfaces of B_4C-30 vol% TiB_2 composites PECS with a degassing step at 1400, 1700, 1900 and 2000 °C, as well as at 2000 °C without a degassing step.

1700 and 1900 °C (Fig. 4a) whereas it was not measured on the ground surfaces (Fig. 4b). The removal of the water-soluble H_3BO_3 on the ground surfaces was due to the presence of cooling water during grinding. The presence of a large amount of H_3BO_3 on the fractured surface implies the presence of B_2O_3 in the ceramics PECS at 1400, 1700 and 1900 °C, since B_2O_3 and humidity water interact immediately on the exposed fracture surface according to an exothermal reaction with the formation of H_3BO_3. The amount of H_3BO_3 decreased with increasing PECS temperature and completely diminished at 2000 °C when applying a degassing step. In contrast to the TiB_2–B_4C composite obtained after PECS at 2000 °C with degassing cycle, the ceramic without degassing cycle contained a substantial amount of graphite, as shown in Fig. 4a and b.

Secondary and backscattered electron micrographs of the starting powder mixture and B30T composites PECS with a degassing step below 2000 °C are presented in Fig. 5. In all ceramics, the bright TiO_2/TiB_2 and grey B4C contrast grains are homogeneously distributed. The starting powder contains submicrometer grained TiO_2 and B_4C powder as well as nanometric carbon black. The ceramic PECS at 1400 °C has nanometer sized TiB_2 grains due to the short reaction cycle. Increasing

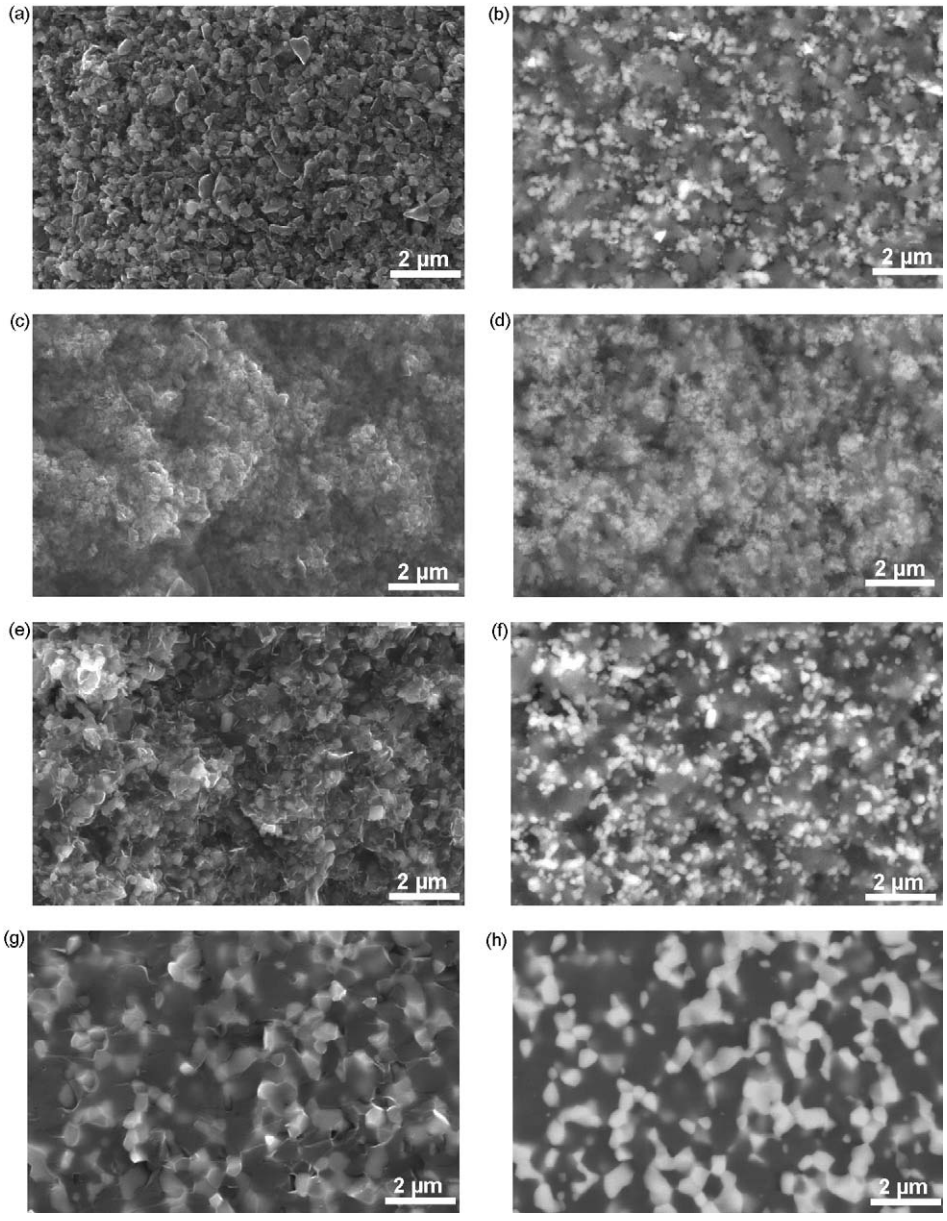

Fig. 5. Secondary (left) and backscattered (right) electron micrographs of the starting powder mixture (a, b) and fracture surfaces of the composites PECS at different temperatures with degassing step, 1400 (c, d), 1700 (e, f) and 1900 °C (g, h).

the temperature to 1700 °C resulted in rapid TiB_2 grain growth. At 1900 °C, relatively large submicrometer and equiaxed TiB_2 grains were evenly distributed in a grey B_4C matrix.

The microstructure of the B30T composites PECS at 2000 °C with and without degassing step are compared in Fig. 6a–d. From the fracture surfaces, both composites can be classified as fully dense. However, the microstructure as well as the phase composition (see Table 1) is significantly different. Graphite flakes (Fig. 6a) were clearly observed in the composite PECS without degassing step. With degassing step during PECS at 2000 °C, the microstructures of B30T (Fig. 6c and d) and B15T (Fig. 6e and f) exhibited equiaxed bright submicrometer TiB_2 grains in a submicrometer sized B_4C matrix.

The chemical composition of the starting powder and composites PECS with a degassing step were measured by SEM-EDS standardless analysis, carried out at 12 kV. As shown in Fig. 7, the B30T starting powder and the ceramics PECS at 1400 and 1700 °C contain a substantial amount of oxygen of about 16.5 wt%. With increasing PECS temperature to 1900 and 2000 °C, the residual oxygen level decreased to 2.46 and 0.3 wt% respectively. When the powder compact was sintered at 2000 °C without a degassing step, a total O content of 8.4 wt% was measured. The oxygen analysis clearly indicated that only the material PECS at 2000 °C with a degassing step resulted in a pure B_4C–TiB_2 composite.

Besides the O level, the C and B content in the composites thermally treated at 1400 and 1700 °C were comparable with that of the starting powder, implying there was no O, C or B containing volatile species formation at these temperatures (see Fig. 7). With a degassing step at 1900 and 2000 °C, the O and C

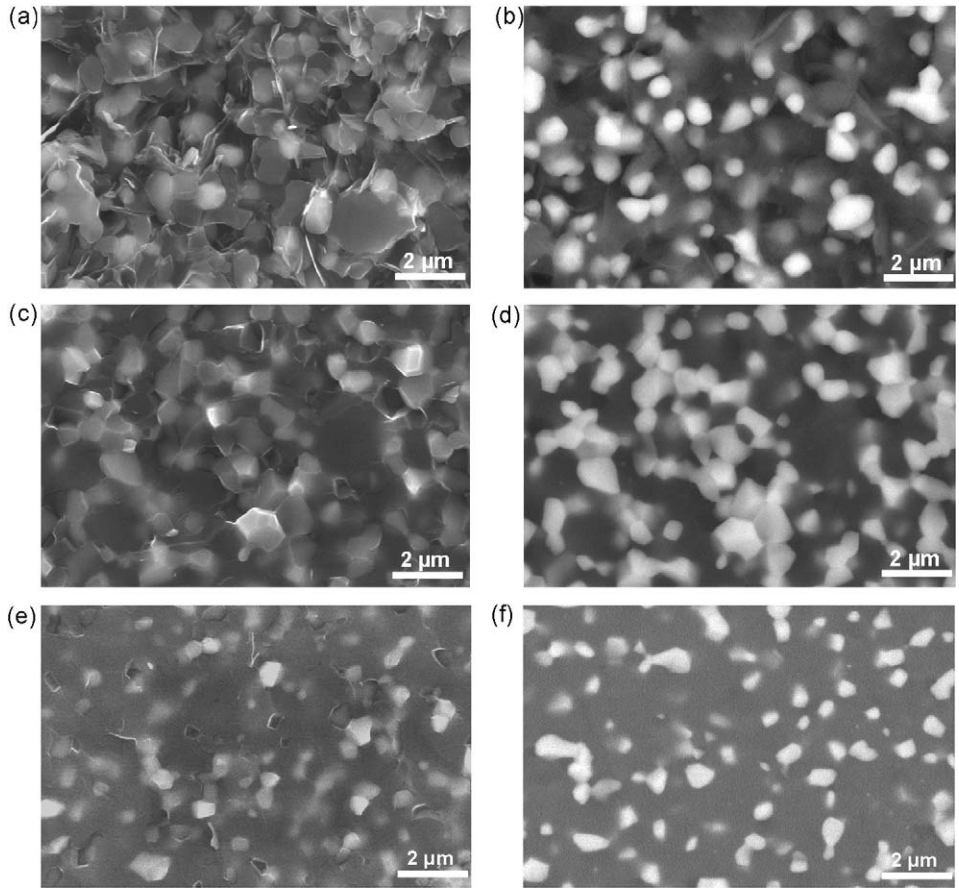

Fig. 6. Corresponding secondary (left) and backscattered (right) electron micrographs of the 30 vol% TiB_2 composites PECS without (a, b) and with (c, d) degassing at 2000 °C, and the 15 vol% TiB_2 composite processed with degassing at 2000 °C (e, f).

content dropped rapidly, whereas the B content increased. The simultaneous decrease in C and O content indicates the release of CO gas when heating to 1900 and 2000 °C. A small amount of Zr originated from the ZrO_2 milling medium.

Based on the phase constitution, the overall composition changes and vacuum pressure evolution, B_2O_3 and graphite were identified as intermediate products during the in situ PECS synthesis of B_4C–TiB_2 composites. TiO_2 initially completely reacted with B_4C forming TiB_2, B_2O_3 and carbon at 1400 and 1700 °C. At 1900 and 2000 °C, the in situ formed B_2O_3 reacted with C forming B_4C and CO gas. When the high temperature reaction was not completed or inhibited by gas entrapment, the liquid B_2O_3 solidified after cooling and readily reacted with water to form H_3BO_3 on the surface when exposed to ambient humid air.

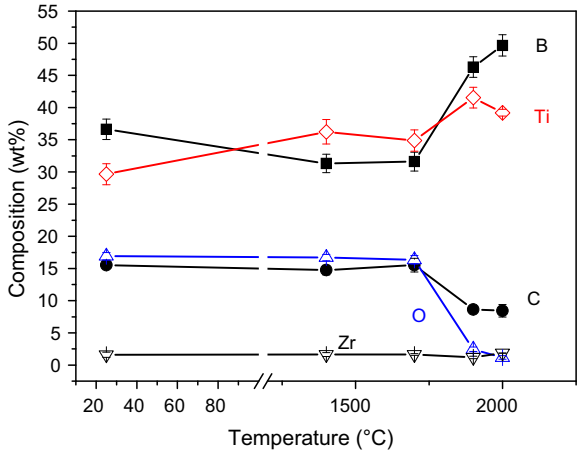

Fig. 7. Standardless SEM-EDS analysis of the B30T starting powder and composites PECS with a degassing cycle.

Direct reduction of TiO_2 or ZrO_2 powder with B_4C has been reported to produce diborides and diboride-carbide composites.[14–17] The reactions between oxides and B_4C are endothermic and become favourable at temperatures lower than for the equivalent reactions with carbon.[17] The reaction of oxides and B_4C has also been exploited to promote the densification of B_4C and ZrB_2 based on the ability of B_4C to react with oxides thereby reducing the amount of oxide impurities.[14,15,21–24] A B_4C-40 wt% TiO_2 mixture without free carbon addition was transformed into a 95% dense B_4C–TiB_2 composite when pressureless sintered for 1 h at 2160 °C.[14] Thermodynamic analysis of the B_4C–TiO_2 system and its experimental verification indicated that TiO_2 is reduced by carbon originating from the B_4C phase, resulting in a mixture of sub-stoichiometric boron carbide and TiB_2.[14] Formation of TiB_2 in a B_4C-50 wt% TiO_2 mixture was observed when thermally treated above 1600 °C.[15]

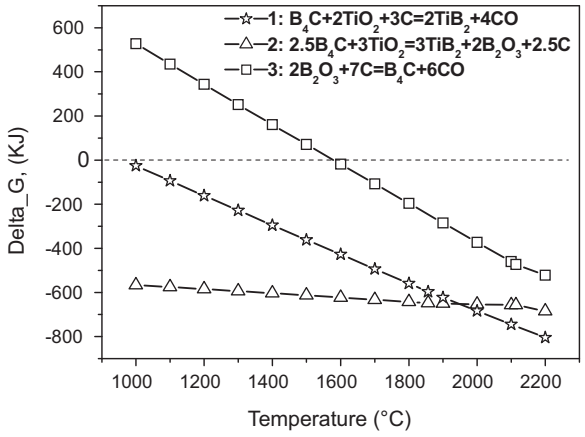

Fig. 8. Change in Gibbs free energy of reactions (1)–(3) as a function of temperature.

In the current PECS experiments, the possible reactions between B_4C, TiO_2 and C forming TiB_2 are:

$$2.5B_4C + 3TiO_2 \Leftrightarrow 3TiB_2 + 2B_2O_3 + 2.5C \quad (2)$$

$$2B_2O_3 + 7C \Leftrightarrow B_4C + 6CO \quad (3)$$

The temperature dependency of the Gibbs free energy change of reactions (1), (2) and (3) under standard conditions is compared in Fig. 8, as calculated by software FactSage.[25]. Reaction (1) is a direct combination of reactions (2) and (3). Under standard state conditions, synthesis of TiB_2 from B_4C and TiO_2 is thermodynamically favourable above room temperature, while the theoretical initial formation temperature of B_4C from B_2O_3 and C is 1580 °C (reaction (3)). Boron carbide powder formation by boric acid or boron oxide reduction with graphite or petroleum coke at 2200–2500 °C has been reported.[24]

In the present experiments, the in situ formed liquid B_2O_3 reacted with C forming B_4C and a substantial amount of CO that causes the vacuum drop during the dwell period at 2000 °C. Due to the presence of extra C in the starting powder, all residual B_2O_3 was converted to B_4C.

In this study, the vacuum pressure in the PECS furnace was maintained around 4 mbar. Under these conditions, liquid B_2O_3 should already start boiling and escape from the powder compact around 1100 °C. However, the logged vacuum level did not indicate any sign of volatilization during the synthesis of the B_4C–TiB_2 composites at 1400 and 1700 °C with a degassing step. Even in the PECS cycle without degassing step (cycle C1) at 2000 °C, only a slightly increased vacuum pressure was detected around 2000 °C (see Fig. 2). Obviously, the volatilization of boron oxide is significantly delayed during the PECS process at lower temperatures, what can be attributed to the fact that the powder compact is relatively insulated from the furnace environment. The graphite papers in-between the punches and the die can temporarily seal off the actual powder compact from the surrounding vacuum vessel. Moreover, a small 30 mm diameter and 4 mm thick sample is PECS in a large vacuum container (about 0.5 m^3) at a heating rate of 200 °C/min. The response of the vacuum pressure measurement is delayed, i.e. vacuum changes seem to appear at a higher temperature during the heating section, due to the vacuum measurement in the exhaust pipe of the system towards the vacuum pump and the high heating rate.

3.2. *In situ fully densified B_4C–TiB_2 composites*

Providing a proper degassing step is included during in situ PECS processing, fully dense B15T and B30T composites can be obtained at 2000 °C. The microstructures of these composites are shown in Figs. 6c–f. The volume fraction of the in situ synthesized TiB_2 phase was estimated by image analysis to be 16.6 and 33.5 vol% respectively on the fractured surfaces of the PECS B15T and B30T composites, which is close to the targeted compositions of 15 and 30 vol%. Compared to hot pressed[4] composites obtained from mixed TiO_2, B_4C and C, or PECS[13] composites from milled Ti, B and C, a much finer microstructure was obtained in the currently investigated PECS composites. The average grain size of B_4C and TiB_2 in the fully dense B30T composite is 0.97 and 0.63 μm, whereas the grain size changed to 1.22 and 0.49 μm respectively when the TiB_2 content was decreased to 15 vol%. Obviously, the growth of the B_4C matrix phase is inhibited by the dispersed TiB_2 phase. TiB_2 grain growth in B_4C–TiB_2 composites is reported to occur mainly through diffusion along the B_4C grain boundaries.[4] Due to the presence of uniformly dispersed TiB_2 grains, B_4C grain boundaries are pinned, hereby inhibiting B_4C grain growth. On the other hand, TiB_2 grains tend to grow when an interconnected TiB_2 grain structure is formed in the B30T composite. This pinning effect is similar to that observed in hot pressed TiB_2–B_4C.[5]

The Vickers' hardness, elastic modulus, indentation fracture toughness and three-point flexure strength were measured for the dense B_4C–TiB_2 composites. The E-modulus of the B_4C-15 vol% TiB_2 composite was 482 GPa and increased to 497 GPa with increasing TiB_2 content to 30 vol% due to the higher intrinsic E-modulus of pure TiB_2. The 30 and 15 vol% TiB_2 composites had a Vickers hardness (HV_1) of 39.3 and 36.9 GPa respectively. Although B_4C is harder than TiB_2, the higher hardness of the 30 vol% TiB_2 grade is due to the refined B_4C grain size. The fracture toughness of the 15 vol% TiB_2 composite was 2.5 MPa $m^{1/2}$ and slightly increased to 3.0 MPa $m^{1/2}$ for the 30 vol% TiB_2 composite.

The measured toughness values are lower than reported for micrometer grain sized B_4C–TiB_2 composites obtained by hot-pressing,[4] 6.1 MPa $m^{1/2}$ at TiB_2 and B_4C grain sizes up to 5 μm, or PECS,[13] 5.9 MPa $m^{1/2}$ at a TiB_2 and B_4C grain size of 1–2 and 5–7 μm, respectively. The toughness data however are in excellent agreement with those reported for finer grained reaction hot pressed B_4C-15 vol% TiB_2 that show a slight increase from 2.7 to 3.7 MPa $m^{1/2}$ with increasing TiB_2 grain size from 0.75 to 2.2 μm.[5] The modest toughness of the present composites is due to their fine grained microstructure and the concomitant limited contribution of crack deflection toughening. An excellent flexural strength of 720 MPa was obtained for the B_4C-15 vol% TiB_2 composite. Due to a finer grain size and homogeneous microstructure, the strength of the 30 vol% TiB_2 composite was even higher reaching an excellent value of 865 MPa.

4. Conclusions

The present study showed that rapid sintering by PECS is a promising route for the preparation of fine-grained in situ synthesized and densified B_4C–TiB_2 composites from TiO_2, B_4C and carbon black powder mixtures. Thermodynamic and experimental assessment of the reduction of TiO_2 with B_4C and C revealed that TiO_2 initially reacted with B_4C to form TiB_2, B_2O_3 and C. The in situ formed B_2O_3 is subsequently reacted with free C to produce B_4C and CO gas. Full conversion of TiO_2 into TiB_2 could be obtained after 7 min at 1400 °C, but complete removal of residual oxygen from B_2O_3 requires a temperature above 1900 °C.

Full composite densification could only be realised when applying an optimized loading cycle in which the maximum load is applied after completion of the in situ B_4C–TiB_2 powder synthesis, allowing degassing of volatile species.

The obtained submicrometer grain sized B_4C composites with 15 and 30 vol% TiB_2 combined a very high hardness of 36.9 and 39.3 GPa with an excellent flexural strength of 724 ± 54 and 865 ± 58 MPa and E-modulus of 482 and 497 respectively. The fracture toughness however is modest and about 2.5–3.0 MPa $m^{1/2}$.

Acknowledgements

This work was performed within the framework of the Research Fund of K.U. Leuven under project GOA/08/007 and the Fund for Scientific Research Flanders under grant number G.0305.07. K. Vanmeensel thanks the Fund for Scientific Research Flanders (FWO) for his post-doctoral fellowship.

References

1. Kim DK, Kim CH. Pressureless sintering and microstructural development of B_4C–TiB_2 based composites. *Adv Ceram Mater* 1988;**3**:52–5.
2. Tuffe S, Dubois J, Fantozzi G, Barbier G. Densification, microstructure and mechanical properties of TiB_2–B_4C based composites. *Int J Refr Met Hard Mater* 1996;**14**:305–10.
3. Skorokhod V, Vlajic MD, Krstic VD. Mechanical properties of pressureless sintered boron carbide containing TiB_2 phase. *J Mater Sci Lett* 1996;**15**:1337–9.
4. Skorokhod V, Krstic VD. High strength-high toughness B_4C–TiB_2 composites. *J Mater Sci Lett* 2000;**19**:237–9.
5. Yamada S, Hirao K, Yamauchi Y, Kanzaki S. High strength B_4C–TiB_2 composites fabricated by reaction hot-pressing. *J Eur Ceram Soc* 2003;**23**:1123–30.
6. Srivatsan TS, Guruprasad G, Black D, Radhakrishnan R, Sudarshan TS. Influence of TiB_2 content on microstructure and hardness of TiB_2–B_4C composite. *Powder Technol* 2005;**159**:161–7.
7. Pierson HO. *Handbook of refractory carbides and nitrides; properties, characteristics, processing and applications*. Westwood, New Jersey, U.S.A.: Noyes Publications; 1996.
8. Ramulu M. EDM sinker cutting of a ceramic particulate composite, SiC–TiB_2. *Key Eng Mater* 1988;**3**:324–7.
9. Tomlinson WJ, Jupe KN. Strength and microstructure of electro discharge-machined titanium diboride. *J Mater Sci Lett* 1993;**12**:366–8.
10. Jones AH, Trueman C, Dobedoe RS, Huddleston J, Lewis MH. Production and EDM of Si_3N_4–TiB_2 ceramic composites. *Brit Ceram Trans* 2001;**100**:49–54.
11. Park JH, Lee YH, Koh Y, Kim H, Baek HE. Effect of hot-pressing temperature on densification mechanical properties of titanium diboride with silicon nitride as a sintering aid. *J Am Ceram Soc* 2000;**83**:1542–4.
12. Huang SG, Vanmeensel K, Malek OJA, Van der Biest O, Vleugels J. Microstructure and mechanical properties of pulsed electric current sintered B_4C–TiB_2 composites. *Mater Sci Eng A*; doi:10.1016/j.msea.2010.10.022.
13. Dudina DV, Hulbert DM, Jiang DT, Unuvar C, Cytron SJ, Mukherjee AK. In situ boron carbide–titanium diboride composites prepared by mechanical milling and subsequent spark plasma sintering. *J Mater Sci* 2008;**43**:3569–76.
14. Levin L, Frage N, Dariel MP. The effect of Ti and TiO_2 additions on the pressureless sintering of B_4C. *Metall Mater Trans A* 1999;**30**:3201–10.
15. Kakazey M, Vlasova M, Gonzalez-Rodriguez JG, Dominguez-Patiño M, Leder R. X-ray and EPR study of reactions between B_4C and TiO_2. *Mater Sci Eng A* 2006;**418**:111–4.
16. Fahrenholtz WG, Hilmas GE. Refractory diborides of zirconium and hafnium. *J Am Ceram Soc* 2007;**90**:1347–64.
17. Baharvandi HR, Talebzadeh N, Ehsani N, Aghand F. Synthesis of B_4C–nano TiB_2 composite powder by sol–gel method. *J Mater Eng Perform* 2009;**18**:273–7.
18. Vanmeensel K, Laptev A, Hennicke J, Vleugels J, Van der Biest O. Modelling of the temperature distribution during field assisted sintering. *Acta Mater* 2005;**53**:4379–88.
19. Anstis GR, Chantikul P, Lawn BR, Marshall DB. A critical evaluation of indentation techniques for measuring fracture toughness: I, direct crack measurements. *J Am Ceram Soc* 1981;**64**:533–8.
20. ASTM Standard E 1876–99. *Test method for dynamic young's modulus, shear modulus and poisson's ratio for advanced ceramics by impulse excitation of vibration*. Philadelphia, PA: ASTM Annual Book of Standards; 1994.
21. Kim HW, Koh YH, Kim HE. Reaction sintering and mechanical properties of B_4C with addition of ZrO_2. *J Mater Res* 2000;**15**:2431–6.
22. Goldstein A, Geffen Y, Goldenberg A. Boron carbide–zirconium diboride in-situ composites by the reactive pressureless sintering of boron carbide–zirconia mixtures. *J Am Ceram Soc* 2001;**84**:642–4.
23. Zhang SC, Hilmas GE, Fahrenholtz WG. Pressureless densification of zirconium diboride with boron carbide additions. *J Am Ceram Soc* 2006;**89**:1544–50.
24. Jung C-H, Lee M-J, Kim C-J. Preparation of carbon-free B_4C powder from B_2O_3 oxide by carbothermal reduction process. *Mater Lett* 2004;**58**:609–14.
25. Bale CW, Chartrand P, Degterov SA. FactSage thermochemical software and databases. *Calphad* 2002;**26**:189–228.